Investigation of impact performance of 3-dimensional interlock polymer fabrics in double and multi-angle pass stabbing

Mengru Li, Peng Wang, François Boussu, Damien Soulat

Version of Record: https://www.sciencedirect.com/science/article/pii/S0264127521003282
Manuscript_76437aaf73e08120673860ebc841d40f

Investigation of impact performance of 3-dimensional interlock polymer fabrics in double and multi-angle pass stabbing

Mengru Li[1], Peng Wang [2, 3, *], François Boussu[1], Damien Soulat[1]

[1]*University of Lille, Ensait, Gemtex, F-59000 Roubaix, France*

[2]*University of Haute-Alsace, Ensisa, Lpmt, F-68000 Mulhouse, France*

[3]*University of Strasbourg, France*

* Corresponding author. Tel.: +33 3 89 33 66 48. Fax.: +33 3 89 33 63 39
E-*mail address*: peng.wang@uha.fr

Abstract:

This paper presents the influence of fabric structures and stab angles on single-pass stab impact and the repeated and multi-angle stabbings of 3-dimensional (3D) warp interlock structural fabrics based on the high-molecular-weight polyethylene (HMWPE) yarns. Five kinds of samples with different structures were experimentally tested using the drop weight stabbing impact equipment at the same impact energy. Radar charts are plotted to demonstrate the differences among different parameters to a better understanding and a more global characterization of single-pass stabbing impact. An image analysis methodology of Structure From Motion (SFM) is used to compare the fabric deformation in Z direction after the stabbing tests. Results indicated that fabric structures have significant effects on the stab impact property that the orthogonal/through-the-thickness interlock fabric has a good stab impact resistance. Besides, the fabric with stab angle of 90° exhibited better single-pass stab impact property than the counterparts with stab angle of 0°. More importantly, the double-pass stabbing tests are compared to the ones of the single-pass stabbing which shows that a better condition occurs when the stab angles are identical in each pass.

Keywords: 3D woven fabric; Fibre-reinforced polymer; Stabbing impact; High-molecular-weight polyethylene (HMWPE); Personal protection equipment.

1. Introduction

Due to the restrictions imposed by firearm control legislation and more commonly used of knives in street fights and muggings [1], an increase of life-threatening assaults with knives happened to the policemen and the public, especially in Europe and Asia [2,3]. Demand for materials used for stab-resistant of soft body armour has been gradually issued [4] with the constant need for reducing weight and enhancing performance of soft body armour [5].

Since soft body armour is composed of flexible fibrous material [6], different fabric structures, including unidirectional, two-dimensional (2D) woven and three-dimensional (3D) woven, were used as soft body armour materials. In terms of unidirectional fabric, resins or thermoplastic sheets are used to make collimated filaments be intact [7]. Woven fabrics are still very popular for soft vests which can provide high yarn packing density [8]. As for 2D woven fabric, for example, the stitching method is applied for bonding more layers of 2D fabric together to improve the protection effect [9]. However, both the unidirectional sheets and stitching fabric have their disadvantages, such as inferior inter-laminar fracture toughness. Thus the 3D woven fabric has been considered to fill in the gap.

Although, from the macro shape point of view, there are solid, hollow, shell and nodal 3D woven structures [10], three-dimensional warp interlock fabric (3DWIF) as one of them has been widely investigated in the past few years. Layers of 3DWIFs are connected by a binding warp yarn to ensure greater cohesion [11,12], preserving the integrity of the entire structure. They have good mechanical properties in through-the-thickness direction, better structural integrity, good layer to layer stress transfer [13]. Because of these excellent performances, they have been studied extensively as ballistic body armour. Abtew et al. [14] investigated the 3DWIF made of similar high-performance yarn (Twaron®) against ballistic impact test for female body armour solution. It found that the energy absorption capabilities of 3DWIF and 2D fabric panels with a higher number of layers did not reveal a significant difference. While shaping the intended panel, 3DWIF revealed better mouldability and less recovery behaviour with fewer wrinkle formations. Shi et al. [15] proposed an analytical model to calculate the energy absorption of the 3D orthogonal woven fabric under ballistic penetration of a hemispherical-cylindrical rigid projectile. However, few studies have been reported on the stab-resistance performance of polymeric 3DWIF materials, which are the future materials for the application of personal protective equipment (PPE) due to their high flexibilities and low weights [13,16].

This paper proposed a novel and unique methodology for characterizing the repeated stab resistance of HMWPE 3DWIFs as polymeric protection materials. The motive for this study is to simulate repeated stab impacts with the same energy level at the same location for different architectures. Five different structures were fabricated according to the four main categories of structure: Angle /Through-the-thickness (A/T), Angle /Layer-to-layer (A/L), Orthogonal /Through-the-thickness (O/T), Orthogonal /Layer-to-layer (O/L). The single-pass stab resistance of different structures was compared and the optimal 3D structure is selected and applied to conduct in-depth research. Moreover, the results of single-pass stab vs. double-pass stab test response of multi-plies 3DWIFs, represented by O-T structures, were compared. An extensive experimental campaign is, thus, developed to compare the repeated stab resistance of multi-plies 3DWIFs, represented by O-T structures, stabbed in different directions. Concurrently, it is expected that the evaluation of stab-resistant performance and behaviour of 3DWIFs can be useful to improve the design of flexible and lightweight fabrics. The methodology presented here can offer an alternative approach for characterizing the repeated stab resistance of HMWPE polymeric fabrics, providing data that is critically needed

to improve the accuracy of stab resistance for the development of more efficient armour and PPE.

To the best of our knowledge, this is the first paper that addresses the double and multi-angle pass stabbing impact of HMWPE polymeric 3DWIFs. The main contributions of this paper can be summed up as follows:

- Improve our understanding of the stabbing impact performance of 3DWIFs manufactured by HMWPE yarn;
- Comparison of the conventional single-pass stabbing impact of different structures' 3DWIFs;
- A novel stab test approach of double and multi-angle pass stabbing impact has been proposed for studying their effect on the stab resistance and the damage of the fabrics, which supplements the lack of testing methods on the classical stab test;
- The contrast between the novel method of double and multi-angle pass stabbing impact and the conventional single-pass stabbing impact is formulated and compared.

2. Relevant literature

Polymeric materials, such as HMWPE [17], are some of the most widely and increasingly used materials in the literature about the development of protection materials due to their low weight, toughness, and excellent resistance to penetration [18–20]. Wang et al. [21] investigated the effects of fabric folding and thickness on the impact behaviour of weave fabric material made of Spectra® 1000 fibres. It was found that the perforation resistance and energy absorption capacity were significantly improved by folding fabric into multiple plies compared to the unfolded counterparts, and the roll-fold fabrics performed best in this study. Min et al. [22] investigated the mechanisms behind the angled ply-orientation on the ballistic performances of multi-ply UHMWPE fabric panels via numerical study. Wang et al. [23] studied the impact behaviour of Dyneema® woven fabric-reinforced laminates with four resin matrices and three thicknesses. The results revealed that the laminates having flexible matrices performed much better in perforation resistance and energy absorption, but had a greater extent of deformation and damage than the counterparts with rigid matrices.

To better understand the stab resistance of fabric or composite panels, researchers often start studying from their structural units [24]. Miao et al. [25] conducted quasi-static stab tests to study the relationships among the stab resistance and fabric density, thickness and the spacer structure. El Messiry et al. [26] demonstrated that Vectran fibre and its triaxial weave fabrics showed higher values of energy absorption compared to the other fibres. Xu et al. [27] indicated the possibility of lighter ballistic panel materials with the use of shear thickening fluids (STF) for higher stabbing protection, as same as Li et al. [28]. However, current research has been emphasized the studies about stab and puncture resistance based upon 2D fabrics or their composite [8], including fabric manufacturing, experimental investigation of stab resistance property, analytical model and finite element method, the STF treatment. Very limited literature issued the application of 3D woven fabrics on stabbing impact.

Whereas the study on 3D woven fabrics mostly focused on the ballistic impact behaviour from analytical modelling and numerical modelling (especially finite element method) approaches [29]. Chu et al. [24] investigated the influences of local and global localizations on the ballistic behaviour of 3D interlock woven fabrics. Ha-minh et al. [30] numerically analysed the effect of friction on the ballistic performance of 3DWIFs. Besides, 3DWIFs are also widely applied as a reinforcement material in the composite for protective material application. Behare et al. [31] observed that 3D interlock fabric reinforced composite shows high stab resistance as compared to the 2D plain woven composite knife penetration test.

Wang et al. [32] studied the drop-weight impact behaviors of 3D angle interlock woven composites after thermal-oxidative aging.

However, it can be noticed that few studies concentrated on the stabbing impact behaviour of dry 3D woven fabric. For example, Dash et al. [33] compared the effect of different stuffer layers and fabric volume fraction on the knife penetration properties of 3D woven fabrics. As another example, Behera et Dash [34] showed that the results of the knife penetration tests are dominant when the linear density of binder tow is coarser, while the impact properties are affected by the number of interlacements in the in-plane region of fabric.

Moreover, all these investigations mentioned earlier paid attention to the conventional characterisation test concerns a single-pass stabbing impact, whether in the part of fibre reinforced polymer fabrics [26] or composites [35–39]. According to the report [40], the victims are suffering not only the single-pass stab wound but also repeated stabs, which might directly result in death. Radojevi et al. [41] studied that 14.36 % of all the 766 cases of homicides were achieved by repeatedly stabbing the victim. In the rapid and close repeated or multiple stab attacks, due to motive and muscle inertia, the stab locations will be very close or even the same. Repeated stabs or double stabs might occur to the same body armour at the same locations, which, to the authors' knowledge, have not been thoroughly investigated in the literature. The classical characterisation of single stab resistance of PPE cannot reflect the real conditions (repeated-stabbing in each pass) considering the movement of the assailant and victim. Therefore, the repeated stabbing test with different stab angles as one type of new low-velocity impact property of 3DWIFs is essential to deeply understand fabric behaviour under multi-hit. It may be that the stabbing attack in homicide is not so accurate, but if the stab resistance under this kind of extreme conditions is enough for protection and then the protection performance under ordinary conditions will be better.

3. Materials and methods

3.1 Materials for testing

HMWPE (Spectra®, Honeywell Company, USA) of 1350 dTex yarns were used to fabricate the polymer 3DWIFs. The inherent tensile strength and cut resistance of high-performance fibres, such as para-aramids and HMWPE, make them good candidates for the construction of flexible, stab-resistant materials [42]. Our previous work [43] showed that the strength of high-performance fibre yarns can be improved by a slight twist. Therefore, the value of 50 twists per meter ("Z" type twist) was applied on the HMWPE yarns both in the warp and weft directions. Table 1 shows the main parameters of HMWPE yarns.

Table 1

The main parameters of HMWPE [44].

Linear density (Tex)	Ultimate Tensile Strength (GPa)	Modulus (GPa)	Elongation (%)	Breaking Strength (N)	Density (g/cm^3)
135	2.57	73	3.9	351	0.97

Five different 3DWIF structures have been designed and produced, according to the four main categories of structure: Angle/Through-the-thickness (A-T), Angle/Layer-to-layer (A-L),

Orthogonal/Through-the-thickness (O-T), Orthogonal/Layer-to-layer (O-L). These fabrics have the same weaving warp density (10 ends/cm) and weft density (40 picks/cm). The fabrics were woven with the help of two warp yarn beams: one is for stuffer warp yarns (0°) and the other is for binding warp yarns (0°), which are interlaced with weft yarns (90°). For all the fabrics, the thickness (NF EN ISO 5084) and the areal density (NF EN 12127) have been measured according to their respective standards. The geometrical structure parameters of five 3DWIFs have been shown in Table 2. In Table 2, both the red and blue yarns of the weft cross-section view are binding warp yarns. One of the yarns is marked as red to see the location of the binding warp yarn in the fabric structure.

Table 2

The geometrical structure parameters and specifications of five structures fabrics.

Fabrics	F1	F2	F3	F4	F5
Structures name	A-L 3-2 4 Binding {Twill 4 effect left}-Stuffer	O-L 3-2 4 Binding {Twill 4 effect left}-Stuffer	A-L 5-3 4 Binding {Twill 6 effect left}-Stuffer	O-T 5-4 4 Binding {Twill 6 effect left}-Stuffer	A-T 5-4 4 Binding {Twill 6 effect left}-Stuffer
Weft cross-section	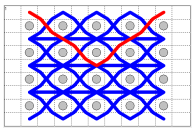	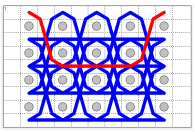	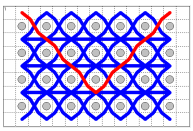	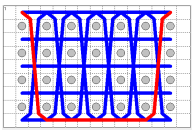	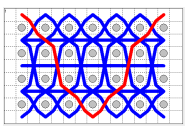
3D views	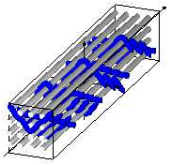	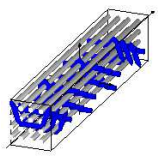	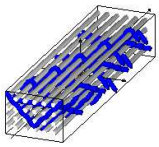	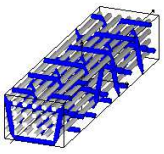	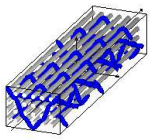
Warp density Weft density			10 ends/cm 42 ends/cm		
Thickness (mm)	2.5±0.3	2.1±0.1	1.9±0.1	1.7±0.1	1.6±0.1
Areal density (g/m^2)	735.8±36.5	720.0±12.3	688.7±13.2	710.6±12.2	714.1±9.6
Fibre volume fraction (%)	30.3±1.5	35.3±0.6	37.4±0.7	40.7±0.7	46.0±0.6

3.2 Dynamic stab resistance test

Fig. 1 shows the schematic of a stab test device used in the present study to characterize the stab resistance. The principle of drop-weight impact [45] (knife fall under the influence of gravity) was used, as shown in Equation below which can derive the falling height h required to generate stab energy.

$$E_P = m \times g \times h$$

Where E_P is potential energy, m is the mass of the knife with the holder in kg, g is the gravitational acceleration and h is the falling height.

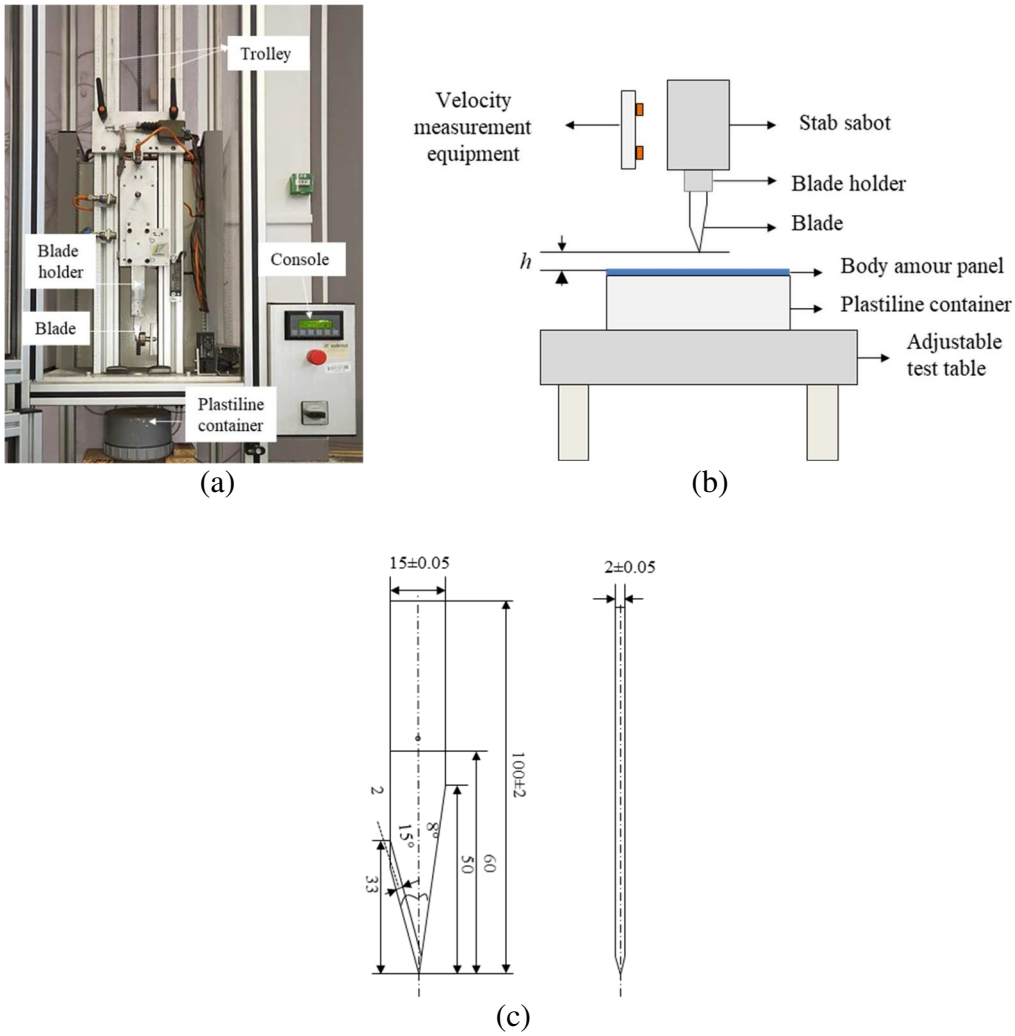

Fig. 1. (a) Drop weight stab impact apparatus; (b) Schematic diagram of stab test device and (c) Details of the stab blade (dimensions in mm).

The kinetic energy of the impactor can be adjusted varying the height *h*, which is measured as the distance between the tip of the blade and the surface of samples lied on the Plastiline® container, as shown in Fig.1. Due to the Plastiline® can keep the print of an impact, it allows simplifying the work without requiring the use of a high-speed camera to assess the impact process [46]. The drop-weight *m* is 2.11kg which is the total mass of the system (stab sabot, blade holder, and blade, Fig.1 b). HOSDB/P1/B sharpness blades (Fig.1c), as engineered test knife that has been designed to replicate the broad spectrum of knives used in assaults on police officers, were proposed in the test indicated in the UK standard [47]. But for the ensuring of steady conditions, each knife has been used a maximum of 10 times since the effect of repeated use of test blades is seen to be relatively small [48]. Besides, the Roma Plastiline® in each tray shall be manipulated to avoid any air gaps before starting to do tests. Once the striker was positioned at the corresponding initial height to achieve the desired stab

energy, it dropped in a free-falling process. The preliminary tests showed that all the fabrics with 1, 3, …,6 plies fabric panels are penetrated completely by the blade with a falling height of 1.16 m according to the standard for the potential energy of 24 J. Besides, it was observed that there is no significant difference of depth of penetration (DOP) among these structures under same fabric panels because the blade was stopped and blocked by the blade holder (shown in Fig.1 (a)) rather than the fabric panels. To find out differences between the different structures fabrics, tests were performed under the energy of 2.5 J in this paper. Note that this energy is lower than that considered in the standards of personal protection analysis; this is because, in this work, the multiple plies of 3DWIFs are analysed under low-velocity stab test and not a real vest. To achieve the protection required by the standard, the improvement in fabric density and the number of layers strongly affected the stab resistance [49,50]. Reiners [48] has found that, after evaluating the penetration depth, there is no significant difference in the results between the sample sizes and there is no significant influence of the pretension onto the results. Specimens have a size of 100 × 100 mm^2. To imitate the human body temperature for the practical application, the Plastiline® containers are kept to the temperature of 37.5 ± 0.5 °C before tests. According to the standard, tests are repeated three times for each sample [47]. Moreover, the reasoning behind the research approach for repeated impacts using the same energy level is discussed. Table 3 shows the conditions for stab resistance testing.

Table 3
The conditions for drop tower testing.

Parameters	Value
Strike energy	2.5 J
Drop mass (m)	2.11 kg
Drop knife type	HOSDB/P1/B
Drop height (h)	121 mm
Gravitational acceleration (g)	9.81 m/s^2
Stab impact velocity	1.54 m/s
Dimensions of the specimen	100 × 100 mm^2

2.2.1 Classical stabbing test

The classical stabbing test concerns the stab-resistant characterization through the single-pass stabbing experiments. Fig. 2 shows schematically the single-pass stabbing experiments (classical stabbing test). The unclamped specimens were located on the top of a Plastiline® container and were aligned to face the stab in the centre of the sheets. The X (0°), Y (90°), Z orthogonal coordinate system is used in describing the stab angle (θ) of the fabric panels. One, three and six plies of 3DWIFs are prepared and laminated. Since the blade is fixed in the

machine, the fabric panel is rotated counter-clockwise to change the relative position of the blade and the fabric. For example, when the blade is parallel to the weft yarn, the stab angle is 0°.

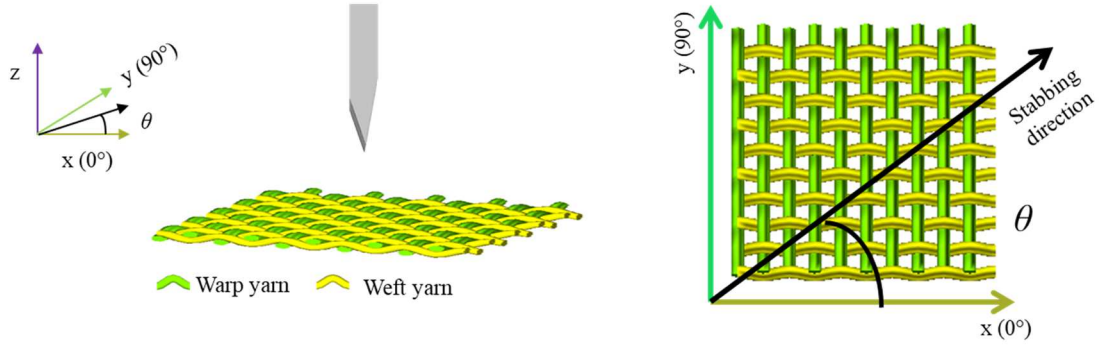

(a) (b)

Fig. 2. A schematic showing the coordinate system of fabric panel (a) 3D schematic diagram, (b) 2D schematic diagram.

To quantify the stabbing deformation in both single-pass and double-pass stabbing tests, three stages of knife attack have been identified [8,51,52], including indentation, perforation and penetration. While, in some cases, there are only two steps, indentation and perforation, of stab-resistant materials that they do not been penetrated by the knife during the stabbing impact. Stab-resistant materials and bulletproof materials have similar functions for protecting the human body from harmful projectiles. However, the mechanism of stab-resistant behaviour is much more complex than bullet-proof behaviour [2]. According to the low velocity of the impact of the blade, stab-resistant materials should simultaneously be able to stop penetration by sharp point and cutting by blade edge [52][53][54]. It is commonly accepted that textile stabbing involves three different steps: the initial indentation step, the second cutting step caused by a knife-edge, and the third step leading to the destruction of the assembled fibre bundle, as is explained in a recent work of Hejazi et al. [55].

2.2.2 Double-pass stabbing

As presented previously, the double-pass stabbing with different stab angles is more worth being characterized compared to the classical test (single-pass stabbing). It is more suitable for the real condition in view of body protection. The double-pass stabs with the same energy level as the single-pass stab will be proposed to study the effect on the stab resistance of the different architectures. Compared to the classical single-pass stabbing test, for double-pass stab, the second stab of the specimen will be stabbed at the same location as the first pass with the same blade and energy. As shown in Figs. 3a and 3b, the blades are perpendicular to warp and weft yarns respectively in two passes. Moreover, compared to the first pass, keeping the same energy, the stab angle was changed in the second pass stab to simulate the multi-angle stabs (see Figs. 3c and 3d). It is because that the victim can be possibly stabbed in the same location but never through the same stab direction (with the same stab angle) considering the movement of the assailant and victim self.

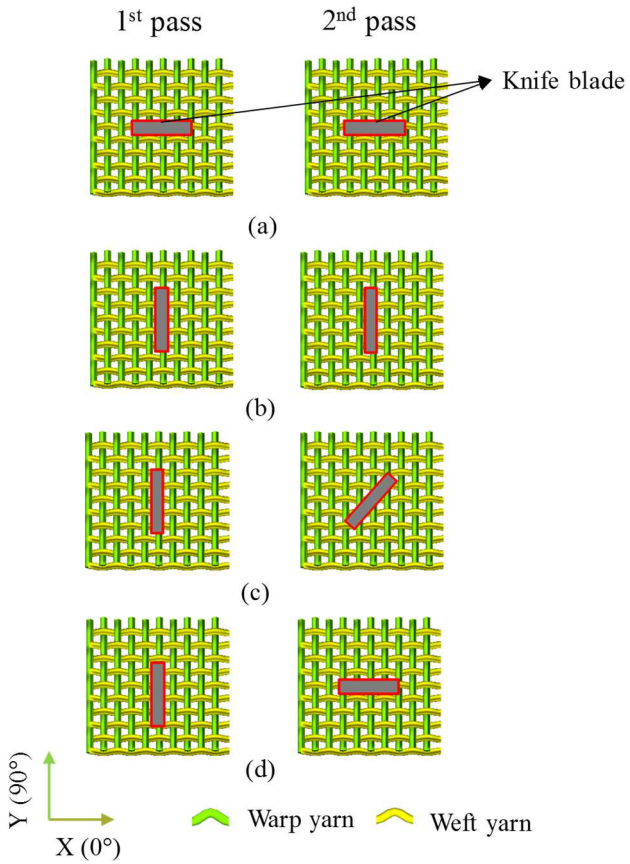

Fig. 3. Double-pass stabbing tests with different stab angles: (a) 0°/0°; (b) 90°/90°; (c) 90°/45°; (d) 90°/0°.

3.3 Measurement of the stabbing deformation

The knife-edge impact on the body protection armour brings out damages or fractures of the specimen that can be delineated in terms of the penetration depth and the number of fabric layers [56]. The stabbing depth can be divided into two parts as shown in Fig. 4a: the depth of penetration (DOP) and the depth of trauma (DOT). The distance between the top tip and the surface of the fabric print mark in the silicone mould is defined as the DOP, which quantifies specially the stabbing trauma. Compared to the DOP, the DOT presents the distance between the surface of the fabric print mark and the bottom of the trauma. To accurately measure and analyse the DOP and DOT, 3D scanning moulding is proposed in the present study (Figs. 4b and 5c).

The RTV 181 poly-condensation silicone as a very resistant elastomer was used to recover prints of the complex shapes of the blade into the Plastiline® (see Fig. 4b). The silicone with a density of 1.25 g/cm^3 was mixed with the catalyst at the ratio of 20:1. The silicone compound was filled into the trauma to obtain the prints of deformation. It is important to force out the air, by using the vacuum oven, to make sure that there are no air bubbles that emerge inside the silicone prints. Once the silicone print is obtained (Fig. 4b), it can be scanned by a 3D scanner and then measured by SOLIDWORKS (Fig. 4c). The 3D shape of the stabbing deformation can be observed and the DOP and DOT can be measured directly with errors less than 0.01 mm.

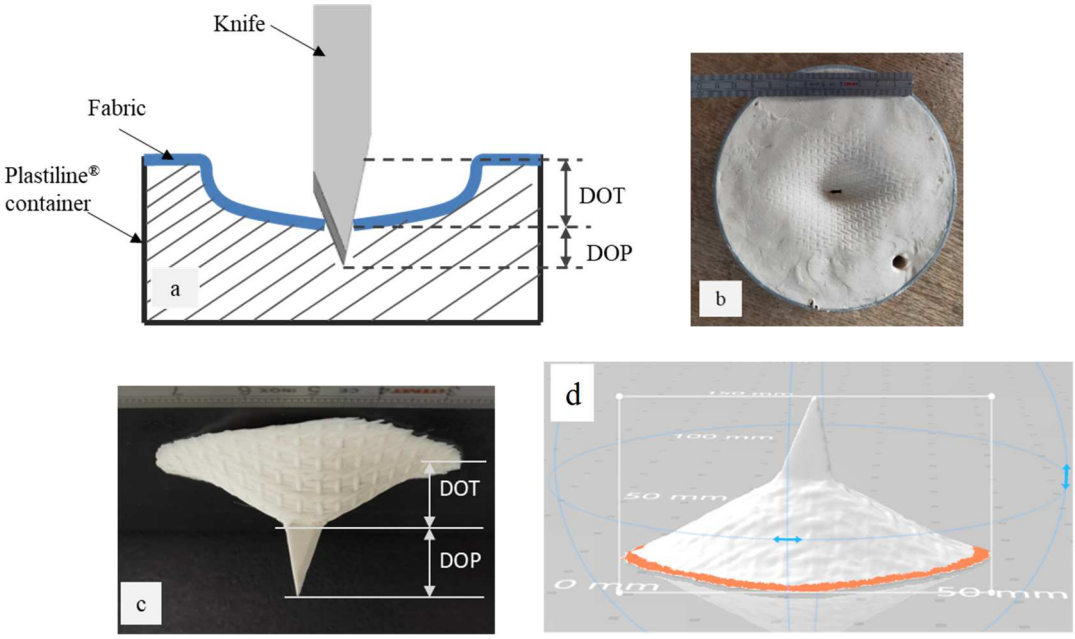

Fig. 4. The stabbing deformation: (a) Definition of the DOP and DOT; (b) Surface state of the Plastiline® after stabbing impact; (c) Silicone print and (d) 3D scanning.

3.4 Image-analysis of deformed fabrics after stabbing test

The Structure From Motion (SFM), as an image analysis methodology originating from computer vision techniques, is used to characterise the deformed fabric shape after the stabbing tests. As described in the study of Shen et al. [57], a stack of photographs, taken around the sample from different angles, were matched by the 3D location of features. Post-processing of the 3D point-cloud of the sample via the SFM method is essential to remove some noise points and improve the quality of modelling with the help of the CloudCompare software. The size of the generated point-clouds was calibrated to real dimensions. Then the differences between two point-clouds from before and after the stabbing test respectively based on Hausdorff distance can be computed [58]. The location and height variation of the deformed fabric is highlighted in the cloud-cloud distance model with an active scalar field. The comparative example between the real sample and model of F4 fabric is shown in Fig. 5. The projection plot of absolute distance in the Z direction (H) between two compared point-clouds (the measured points between before and after the stabbing test) is then given through this method from the top view of the centre shown in Fig. 5c. The regions in red correspond to the parts of deformed fabric further away from the reference fabric (before stabbing impact), and the regions in blue correspond to the parts of deformed fabric are closer to the reference fabric. The accuracy of the method is ± 0.5 mm which is related to the image details, including the surface texture of the target object, the density, sharpness and resolution of the photoset.

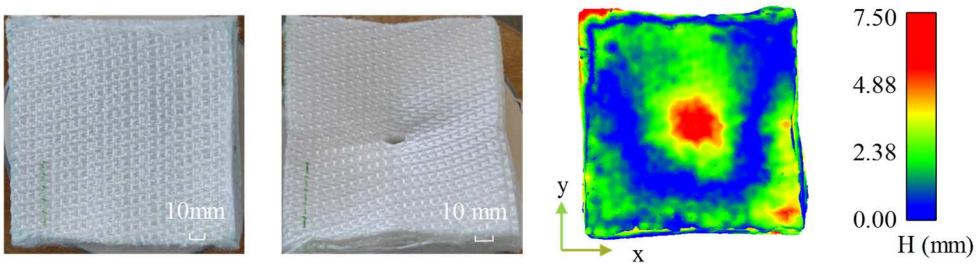

(a) (b) (c)

Fig. 5 Comparative examples between real samples and model, (a) real sample before stab test, (b) real sample after double stab 90°/0 °, (c) sample model after double stab 90°/0 °.

4. Results and discussion

4.1 Single-pass stab resistance

Fig. 6 shows the DOP after the single-pass stabbing tests of different samples. A clear difference can be observed among the five architectures and different laminated plies against the knife (P1) impactor. The DOP of the impact knife into the backing material tends to decrease with the increase of panels number, this phenomenon can be confirmed by the study of Tien et al. [56]. No significant difference of DOP can be noted in the single-pass stabbing with one-ply fabric with a stab angle of 0°. It is obvious that the five fabrics are penetrated completely by the blade and then the blade stopped penetrated due to the knife handle, which is 60 mm from the tip of the blade, was blocked by the fabrics. Therefore, the DOP is approximately equal to the length of the exposed blade for one-ply fabric. Following the increase in the number of plies, the DOP value is reduced. It confirms that the increase in fabric plies has more effect on decreasing the penetration depth.

Moreover, the smaller DOP can be observed in F4 and F5 fabrics than the other three samples (F1, F2, and F3 fabrics). When the fabric plies increase into 6 plies, especially, the DOP value in F4 and F5 fabric is considerably less than other structures. Since these fabrics were manufactured under the same condition, the F1, F2, and F3 fabrics with layer-to-layer interlock fabrics have a relatively loose structure that it is easier for the tip of the knife blade to stab in the gap of fabrics rather than on the yarns of fabrics [59]. By contrast, F4 and F5 fabrics have orthogonal interlock structures where the binding warp yarns are perpendicular to the weaving plane and go through the whole thickness with the largest binding depth.

Although no obvious trend can be noted for the depth of trauma (DOT), it always remains at a weak level for F4 and F5 fabrics (as shown in Fig. 7). Moreover, the asymmetrical V-shaped knife blade has the only one-side cutting edge with 33 mm length which is lower than the DOP value of all the fabric panels, except the six plies F4 and F5 fabrics with the stab angle of 0°. It is probably due to the effect that all the preforms are well penetrated to bring out an important DOP.

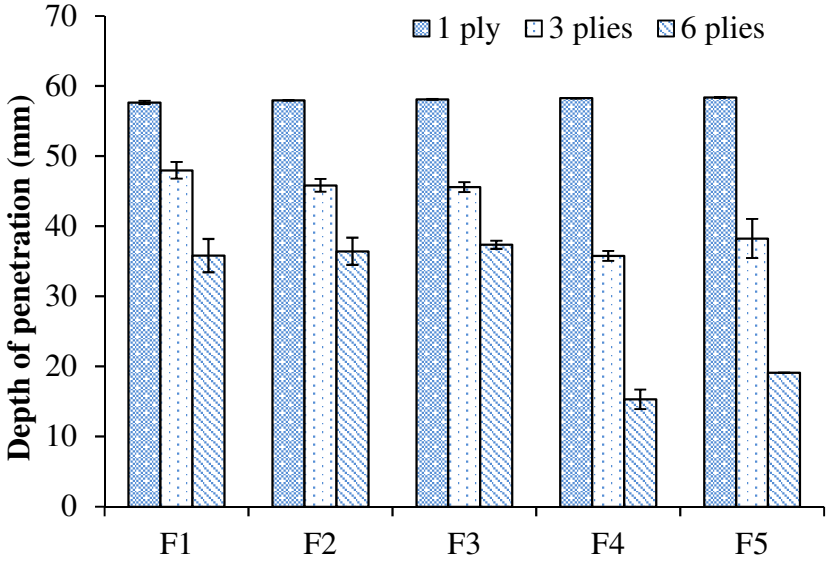

Fig. 6. DOP of different preforms in stabbing tests with the stab angle of 0°.

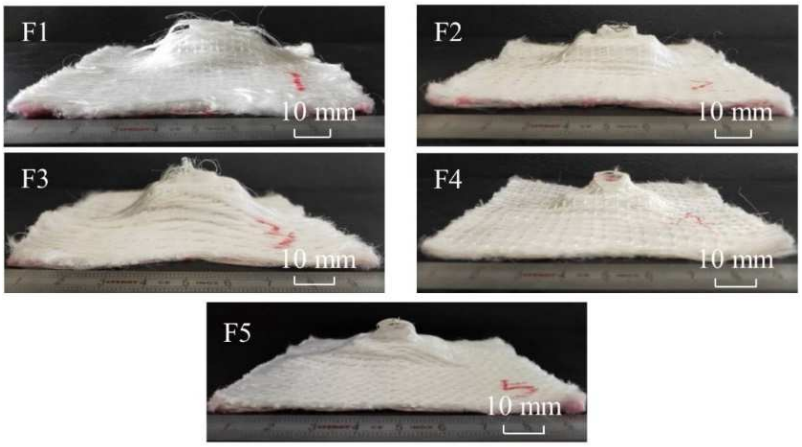

Fig. 7. Observation of the stabbing deformation on the bottom surface in the single-pass stabbing test with 1 ply fabric panel.

The DOP per unit thickness is figured out (Fig. 8) to analyse the influence of fabric thickness on the single-pass stab resistance. Regarding the single-layer samples (1 ply), as the DOP in each stabbing test is superior to 60 mm (the maximum value can be measured by the stab test device, discussed in Fig. 8), the DOP per unit thickness is directly related to the fabric thickness noted in Table 2. F4 and F5 fabrics have more important DOP per unit thickness than other fabrics due to their low layer height. By contrast, the influence of fabric thickness on the stab resistance can be reflected well in the stabbing of multilayered samples. An increase in thickness does make a qualitative difference to the results of DOP, F4 fabric with a low thickness (1.6 mm) has the same or smaller DOP per unit thickness compared to the other fabrics, which indicates a better stab resistance presenting in the F4 fabric structure.

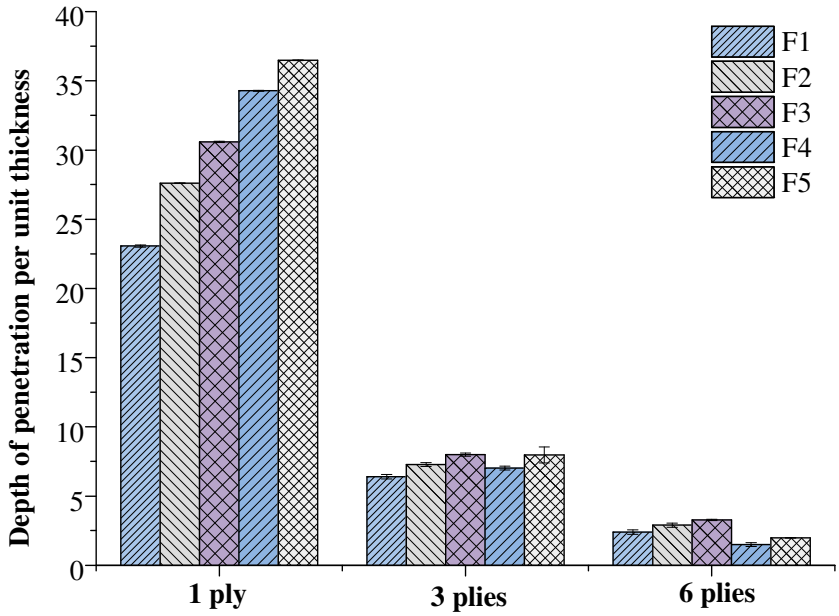

Fig. 8. DOP per unit thickness in stabbing tests with the stab angle of 0°.

The stabbing deformation of the single-pass with the stab angle of 90° was carried out. The comparison with 0° stab angle is figured out for the preforms with 6 plies (Fig. 9). Regarding the F1, F2, and F3 fabrics, the stabbing deformation (DOP) is smaller through 0° than 90°. By contrast, this stabbing deformation is quasi identical in 0° and 90° which can be observed by the damaged area with stab angle of 0° and 90 ° (Fig. 10). Although the sample exhibits almost four times larger weft yarn density than the warp yarn density, the advantage of stab resistance through 90° is not significant than the counterparts through 0° which might be due to the structures of 3D warp interlock fabrics. From the perspective of the thickness direction of the fabric, all the fabrics have four layers of weft yarns, which indicates that the weft yarns density in each layer of the 3D structure is theoretically approximately equal to the warp yarns density. Thus, the gap between the warp and weft yarns in each layer of the 3D structure is theoretically equal. This result shows that yarn density is not the main influence factor. In our previous study [43], the weft yarns crimps are lower than the binding warp yarns crimps. Higher yarn crimps could result in a higher fibre volume fraction in the fabric structure which prevents the knife blade from penetrating the yarn gap. As for the lower weft yarn crimps, it is difficult for the knife blade to stab on all the yarns near the blade and some yarns are likely to be forced out rather than cut. Compared to the F1, F2 and F3 architectures, the DOP is significantly lower for F4 and F5 fabrics in both 0° and 90° stabbing, in particular for F4 fabric (Fig. 9). The F4 and F5 architecture exhibits the highest stab resistance against penetration when compared to the other panels due to their higher fibre volume fraction (Through-the-thickness interlock structure), as the densely-multilayered or closely-spaced laminated preforms can dissipate the energy of an impact [60].

The damage morphologies of 6 plies panels are displayed in Fig. 10, which demonstrates stab damage areas of the F4 and F5 fabrics are lower than that of the F1, F2 and F3 fabrics. As shown in Fig. 10, the dominant failure mechanism is fibre cutting in the middle of the stab position. While some fibres/yarns of F1, F2 and F3 fabrics were also extended and slipped rather than broken. Because the binding type of through-the-thickness causes interlock structures with higher fibre volume fraction than the binding type of layer-to-layer. Besides, in our previous work [43], the binding depths of binding warp yarns from these 3DWIF structures are lower than F4 and F5 fabrics, which indicated that F1, F2, and F3 structures

were fairly loose. Then, in the second stage, i.e. cutting caused by a knife-edge, when there is no more space present for the yarns to extend further, the knife was almost locked up and started to cut the yarns. Comparatively speaking, the edges of cutting areas from F4 and F5 fabrics are relatively smooth. In the third step, F1, F2, and F3 fabrics were damaged with more assembled fibre bundles under the same drop-weight impact energy. It can be proved by the damage observations of the stabbing deformation on the bottom surface of 6 plies fabric panels after single-pass stabbing tests in the stab angle of 0° and 90 ° (Fig. 10).

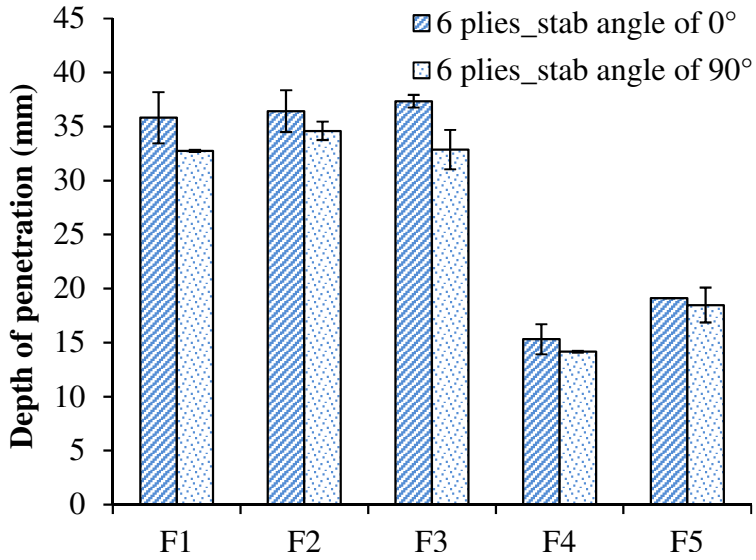

Fig. 9. Comparison of stabbing deformation of 6 plies laminates in single-pass stabbing tests with different stab angles (0° and 90°).

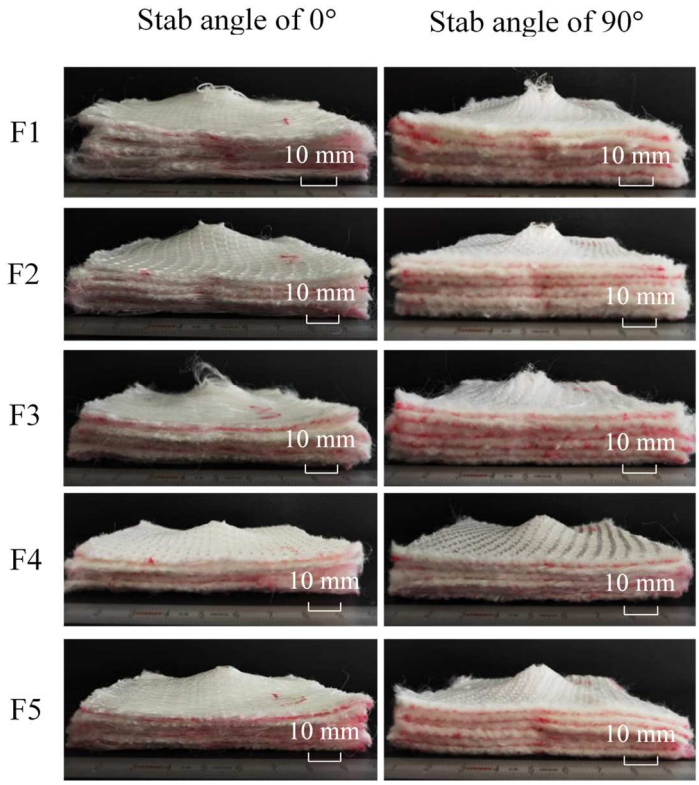

Fig. 10. Damage morphologies of the stabbing deformation on the bottom surface of 6 plies fabric panels after single-pass stabbing tests in stab angle of 0° and 90 °.

To have a better understanding and a global evaluation of stab resistance of different 3DWIFs, a single radar chart diagram is plotted and presented in Fig. 11. Six main indicators of different 3DWIF structures (thickness, areal density, fibre volume fraction, and DOP with stab angle of 0°) are chosen. It can be remarked that F4 and F5 fabrics have smaller DOP values with less thickness and areal density, which shows that these two fabrics (Orthogonal /Through-the-thickness and Angle /Through-the-thickness structures) have better stab resistance with lighter weight and less thickness. It can be also observed that F4 fabric (purple line in Fig.11) covers a smaller area than F5 fabric. In F4 and F5 fabric structures, the Z-yarns (binding warp yarns) run through the thickness direction to hold the stuffer warp yarns and weft yarns together to form a quite stable structure, which can absorb energy more efficiently compared to other interlock structures. Compared to F4 and F5 structures, the differences are the yarn crimps and yarn crimp angles per unit cell of binding warp yarns that are placed through the thickness direction to hold the weft yarns as shown in our previous study [43]. F4 fabric with orthogonal interlock structure has larger yarn crimps and yarn crimp angles per unit cell, which might contribute to increase the yarn frictions and dissipate a portion of the total energy absorption in the fabric during the stabbing. Consequently, in single-pass stabbing, the F4 fabric with O-T structure shows the most desirable stab resistance performance.

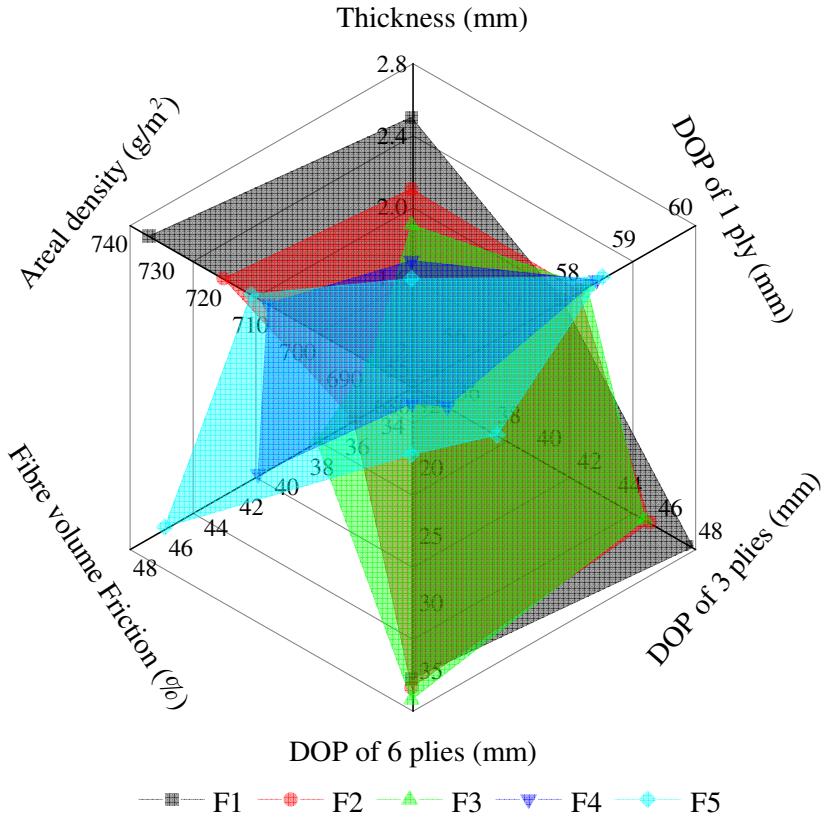

Fig. 11. Summary of different parameters from different fabrics.

4.2 Double-pass and multi-angle stab resistance

The different drops were performed as schematically described in the NIJ standard [12]. Thus, the first drop was performed in the centre of the plastilina block (Fig. 12a), followed by the four other drops closer to the edges of the block (Fig. 12b).

Based on the single-pass stabbing results, the study of the double-pass and multi-angle stab resistance is focused on the F4 architecture. The repeated stabbing should be experienced in the condition in which the perforation or small penetration presents in the first pass (see Fig. 4). Consequently, the panels of sixteen F4 plies are chosen to achieve the investigation. Fig. 12a shows the DOP in double-pass stabbing tests with different stab angles (as mentioned in Fig.3) and the comparison with the single-pass ones through stab angles of 0° and 90°, respectively. No penetration is observed for the single-pass with a stab angle of 90°, which indicates that the P1 blade impactor was blocked and could not penetrate the specimen. Regarding the single-pass in stab angle of 0°, the specimen is penetrated with 0.5 mm depth due to that the weft yarn density (42 picks/cm) is larger than warp yarn density (10 ends/cm). Therefore, cutting in warp direction (in stab angle of 0°) is more easily than in the weft direction (in stab angle of 90°), the effect of the yarn density on the stab resistance is obvious in this case.

From the stabbing results, it can be remarked that the panel of sixteen F4 plies has a great anti-stabbing performance in single-pass conditions but not in certain double-pass ones. Compared to the single-pass results, the DOP has a large increase in double-pass stabbing, in particular in double-pass in stab angle of 90°/45° and double-pass in stab angle of 90°/0° tests. A very similar DOP can be obtained in double-pass in stab angle of 90°/45° and double-pass in stab angle of 90°/0° stabbings, this DOP is two times to the ones in double-pass in stab angle of 0°/0° and double-pass in stab angle of 90°/90° conditions. Therefore, the better condition occurs when the stab angles are identical in the first and second passes.

In addition, the double-pass in stab angle of 90°/90° shows relatively better stab resistance compared to the double-pass in stab angle of 0°/0°. Besides the influence of the yarn density in warp and weft directions, in orthogonal interlock architecture, some warp yarns are deeply bent from one surface to the other, thus preventing slippage of the yarns in the structure while weft yarns follow a smoother evolution. DOT increases in double-pass stabbing than the single-pass one. By contrast with the DOP, the DOT in different double-pass stabbings remains quasi the same level considering the measurement errors (see Fig. 12b). The knife blade causes the compressive yielding of the fabric surface during the first stage of indentation (Fig. 2). Hosfall [52] showed that indentation theory appears to give good agreement with the perforation resistance of sheet materials penetrated by knives. A similar phenomena, in this case, could be supported by an indentation mechanics reviewed by Tabor [61] that, for pyramidal or conical indenters, the plastic zone size is constant relative to the indentation size. In this study, the same knife blades were used with the same tip angle. Therefore, there is a slight difference in DOT values in different double-pass stabbings which showed that it might also be related to the frictional interaction with the fabric panels.

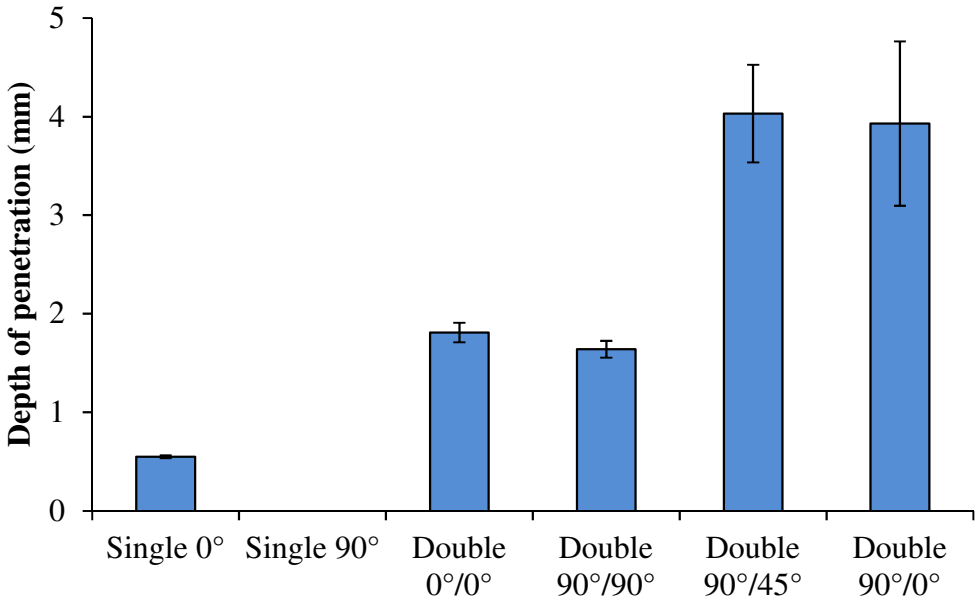

(a) DOP values

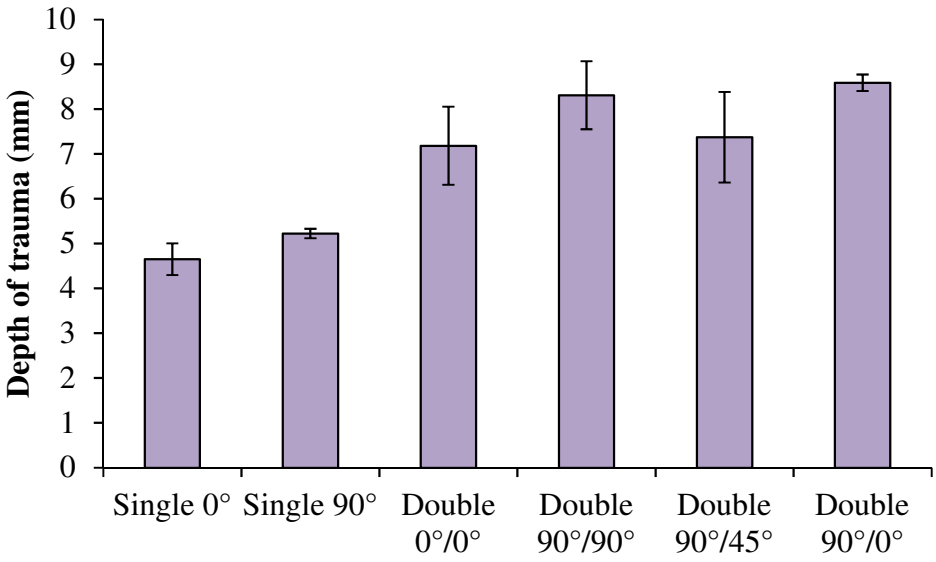

(b) DOT values

Fig. 12. Stabbing deformation after double and multi-angles stabbing and comparison with the single-pass ones.

It was shown in the above experiments that the double-pass stabbing with the stab angle of 0°/0° and 90°/90° shows the relatively better stab resistance compared to the ones with stab angle of 90°/0° and 90°/45°. These phenomena are probably related to the fabric deformation after stabbing. Figs. 13a -13f show the contour plots of the deformation patterns from the top view of sixteen plies F4 fabric after single-pass and double-pass stabbing with the different stab angles. The X and Y axes show the 0° and 90° directions, respectively.

Figs. 13a and 13b present the deformed fabrics after the single-pass stabbing (as same as the first pass in the double-pass stabbing). This kind of deformation is attributed to the fabric structure with tightening yarns that dissipate the impact energy and stop the penetration of the knife blade. Regarding the double-pass stabbing (after the second pass in the double-pass

stabbing) with 0°/0° and 90°/90° shown in Fig. 13c and 13d, the deformation map is similar compared to the one after the single-pass (Figs. 13a and 13b), as the stab angle is not changed between the first and second passes. If the second pass stabbing with the same stab angle and impact energy, the deformed fabric after the first pass stabbing with tightening yarns and structure can resist maximum another impact during the second pass stabbing. In this case, it can be called the deformed state after the first pass stabbing as the "locking" structure. The gap between the yarns reduced and the yarns are gradually in contact with their neighbours [62] during the first pass stabbing impact process, which has resulted in the increase of local areal density. Therefore, it is hard for the knife blade without changing the stab directions to penetrate such kind of deformed and locked fabric unless the impact energy increases enough to unlock the "locking" structure. When the fabric was stabbed the second time, the yarns are completely in contact with their neighbours. Then the fabric reached the "locking" angle and yarns cannot rotate. It is why the low DOP is observed in 0°/0° and 90°/90° double-pass stabbing tests as shown in Fig. 12a. By contrast, when the angle of the second pass stabbing is changed in the double-pass test (e.g. 90°/0° or 90°/45° double-pass stabbing test), the deformation map is strongly modified (see Figs. 13e and 13f) compared to the single-pass stabbing. The changed angle brings out an impact in another direction and consequently leads to other deformed yarns and structures during the second pass stabbing. The "locking" state after the first stabbing is destroyed. Thus the knife blade continues to penetrate and the DOP is bigger compared to the case without changing the stab angle (see Fig. 12a).

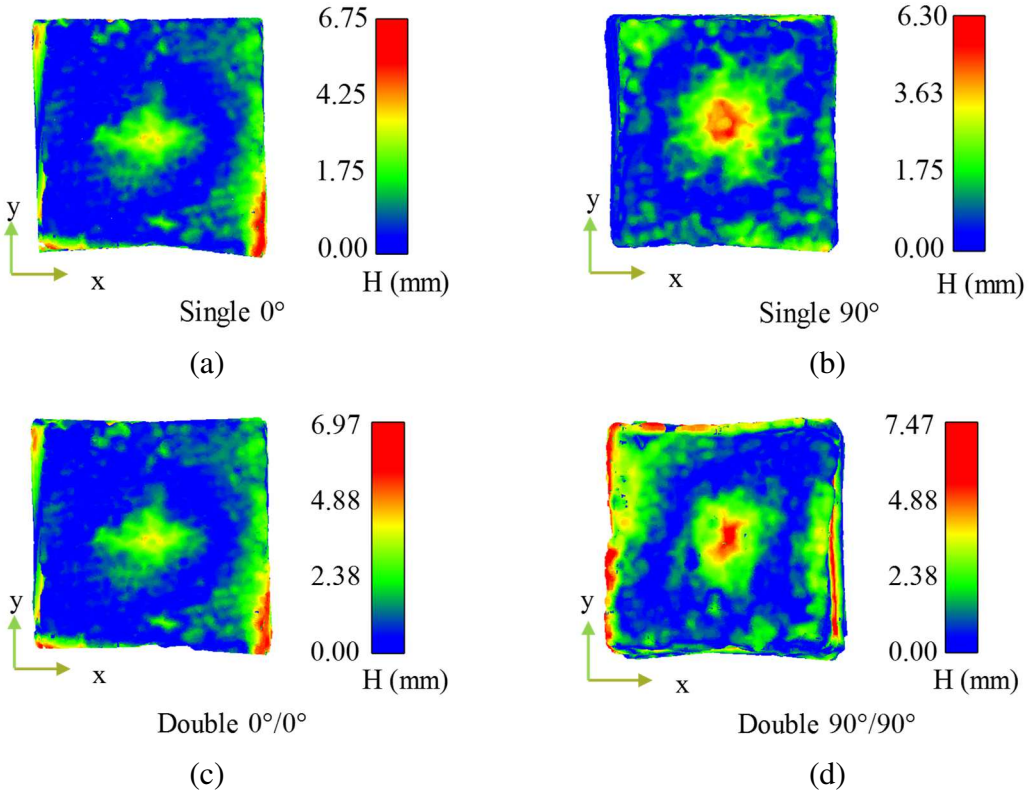

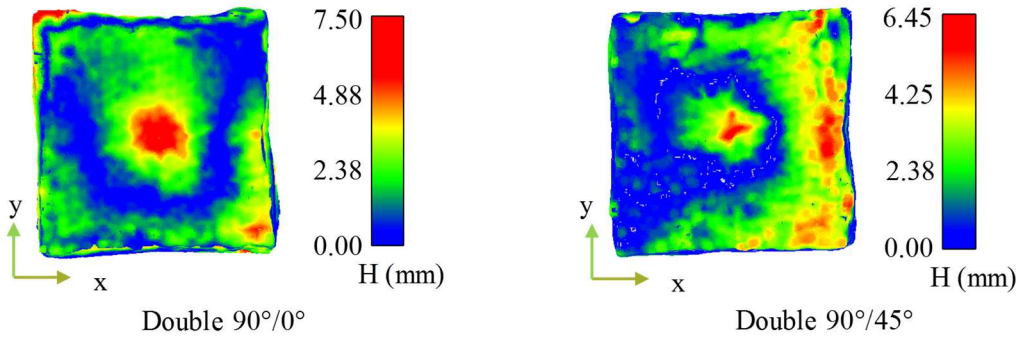

Fig. 13. The sixteen plies F4 fabric patterns from the top view after single-pass and double-pass stab with the different stab angles: (a) single 0°, (b) single 90°, (c) double 0°/0°, (d) double 90°/90°, (e) double 90°/0°, (f) double 90°/45°.

The second stab was carried out by the same blade since a sharp and pointed edge of a weapon remains rigid and unaffected by the impact event [63]. For the double-stabbed specimens, the trauma shape can reveal important information about the nature of the damage that occurred due to the two times stabs. The observation of the bottom surface after different stabbing tests for sixteen F4 plies is shown in Fig. 14. As proved in Fig. 11 a, no or very small penetration presents in single-pass stabbing, quasi no structural damage can be noted in Figs. 14a and 14b. In double-pass stabbings of 0°/0° and of 90°/90° (Figs. 14c and 14d), the shapes of damage are very similar looking like a square-circle one, which is smaller than the structure damages in double-pass stabbings of 90°/0° and of 90°/45° (Figs. 14e and 14f). Moreover, the structure damages with the "triangular" shape in double-pass 90°/0° stabbing and with the "Y" shape in double-pass 90°/45° stabbing are more fatal from the point of view of personal body protection. It confirms again that in the stabbing test the favorable condition is no change of the stab angle in the different stab pass. Consequently, in the real condition in which the change of the stab angle can not be controlled due to the movement of the assailant and victim, the multiaxial balance architecture may be a good solution.

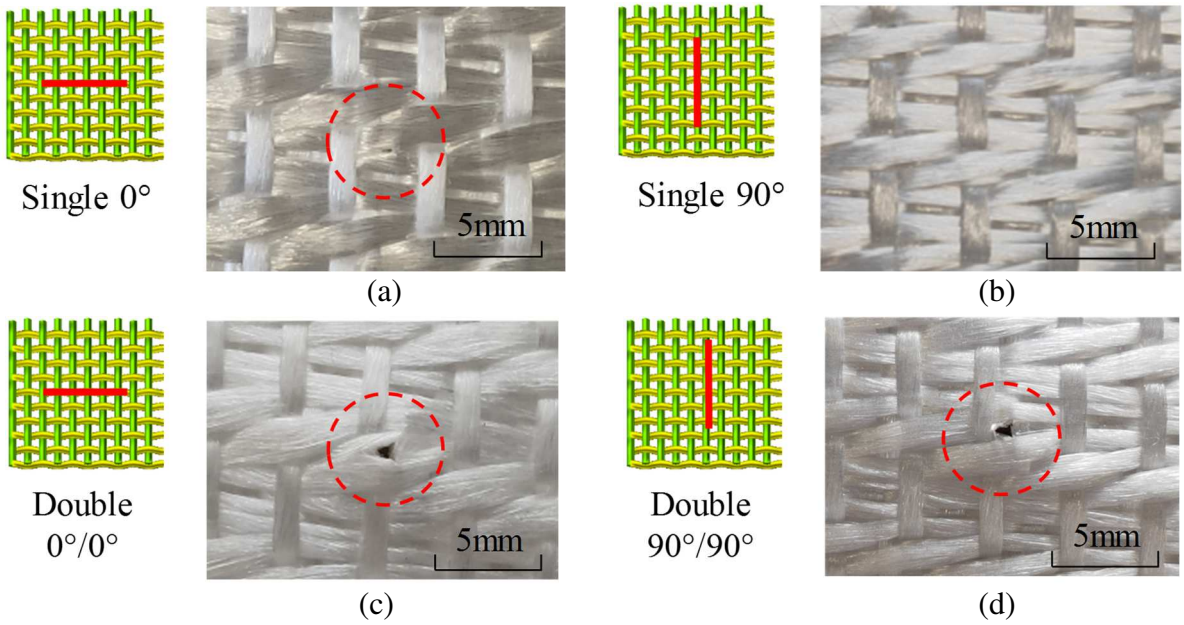

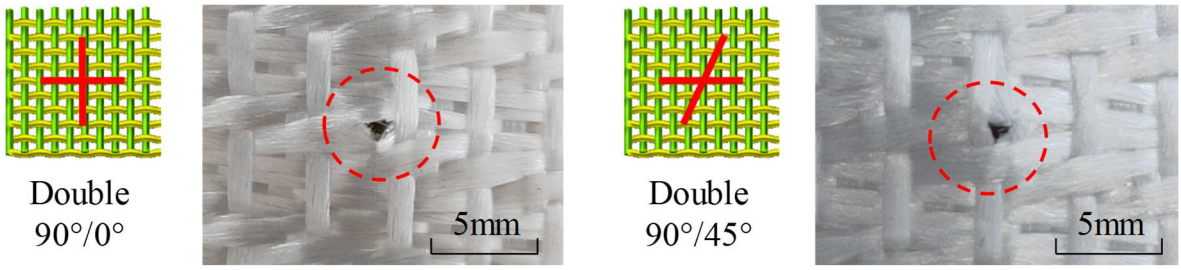

(e) (f)

Fig. 14. Observation of the bottom surface after different stabbing tests for sixteen plies F4 fabrics.

5. Conclusions

Compared to the classical single-pass stabbing impact, the double-pass stabbing impact with different stab angles is proposed and analysed in the present paper to respond more appropriately to the personal body protection problem. Five different structures of 3D warp interlock fabrics were fabricated by HMWPE yarns in the same lab using the same dobby loom to find an optimized fabric structure. All the specimens are stabbed with the same impact energy level and the depth of penetration (DOP) is measured by the 3D scanning method. Based on this study, the following conclusions were made:

- The increase of fabric plies results in the improvement of stab resistance impact of 3D warp interlock fabric panel.
- It is observed from the comprehensive evaluation radar chart that the HMWPE fabric with the Orthogonal/Through-the-thickness (O/T) structure reveals better stab resistance compared to other main 3D warp interlock structures.
- The measurement results of DOP in double and multi-angle pass stabbing provide that the stab resistance in 90° (perpendicular to the weft yarns) is higher than that in other directions.
- The double and multi-angle pass stabbing results highlight also that the better condition occurs when the stab angles are identical in each pass.

As for further study, developing the multi-axial balance Orthogonal/Through-the-thickness (O-T) interlock fabric and studying the third or multiple stabbing impact with higher impact energy in same or different locations are promising to be explored and compared with single-pass and double-pass impact.

CRediT authorship contribution statement

Mengru Li: Investigation, Methodology, Data curation, Formal analysis, Writing-original draft. **Peng Wang:** Project administration, Supervision, Methodology, Data curation, Formal analysis, Writing-review & editing. **François Boussu:** Project administration, Supervision, Methodology, Software, Resources, Review & editing. **Damien Soulat:** Project administration, Methodology, Resources, Review & editing.

Acknowledgment

The authors wish to express their gratitude to the China Scholarship Council (Project no. 201708420167) for financially supporting this work.

References

[1] K.K. Govarthanam, S.C. Anand, S. Rajendran, Development of advanced personal protective equipment fabrics for protection against slashes and pathogenic bacteria part 1: Development and evaluation of slash-resistant garments, J. Ind. Text. 40 (2010) 139–155. https://doi.org/10.1177/1528083710366722.

[2] M.J. Decker, C.J. Halbach, C.H. Nam, N.J. Wagner, E.D. Wetzel, Stab resistance of shear thickening fluid (STF)-treated fabrics, Compos. Sci. Technol. 67 (2007) 565–578. https://doi.org/10.1016/j.compscitech.2006.08.007.

[3] J.P. Henderson, S.E. Morgan, F. Patel, M.E. Tiplady, Patterns of non-firearm homicide, J. Clin. Forensic Med. 12 (2005) 128–132. https://doi.org/10.1016/j.jcfm.2004.10.011.

[4] M. Rodríguez-Millán, A. Álvarez-Díaz, J. Aranda-Ruiz, J. Álvarez-Díaz, J.A. Loya, Experimental analysis for stabbing resistance of different aramid composite architectures, Compos. Struct. 208 (2019) 525–534. https://doi.org/10.1016/j.compstruct.2018.10.042.

[5] X. Chen, Y. Zhou, 6-Technical textiles for ballistic protection, in: Handb. Tech. Text., 2016: pp. 169–192. https://doi.org/10.1016/b978-1-78242-465-9.00006-9.

[6] U. Mawkhlieng, A. Majumdar, A. Laha, A review of fibrous materials for soft body armour applications, RSC Adv. 10 (2019) 1066–1086. https://doi.org/10.1039/c9ra06447h.

[7] N. Hassim, M.R. Ahmad, W.Y.W. Ahmad, A. Samsuri, M.H.M. Yahya, Puncture resistance of natural rubber latex unidirectional coated fabrics, J. Ind. Text. 42 (2012) 118–131. https://doi.org/10.1177/1528083711429144.

[8] R. Nayak, I. Crouch, S. Kanesalingam, J. Ding, P. Tan, B. Lee, M. Miao, D. Ganga, L. Wang, Body armor for stab and spike protection, Part 1: Scientific literature review, Text. Res. J. 88 (2018) 812–832. https://doi.org/10.1177/0040517517690623.

[9] M. Karahan, A. Kuş, R. Eren, An investigation into ballistic performance and energy absorption capabilities of woven aramid fabrics, Int. J. Impact Eng. 35 (2008) 499–510. https://doi.org/10.1016/j.ijimpeng.2007.04.003.

[10] X.G. Chen, Advances in 3D Textiles, 2015.

[11] F. Boussu, I. Cristian, S. Nauman, General definition of 3D warp interlock fabric architecture, Compos. Part B Eng. 81 (2015) 171–188. https://doi.org/10.1016/j.compositesb.2015.07.013.

[12] S.Z. Sheng, S. Van Hoa, Modeling of 3D Angle Interlock Woven Fabric Composites, J. Thermoplast. Compos. Mater. 16 (2003) 45–58. https://doi.org/10.1106/089270503023206.

[13] M. Li, P. Wang, F. Boussu, D. Soulat, A review on the mechanical performance of three-dimensional warp interlock woven fabrics as reinforcement in composites, J. Ind. Text. 0 (2020) 1–50. https://doi.org/10.1177/1528083719894389.

[14] M.A. Abtew, F. Boussu, P. Bruniaux, C. Loghin, I. Cristian, Engineering of 3D warp interlock p-aramid fabric structure and its energy absorption capabilities against ballistic impact for body armour applications, Compos. Struct. 225 (2019) 1–15. https://doi.org/10.1016/j.compstruct.2019.111179.

[15] W. Shi, H. Hu, B. Sun, B. Gu, Energy absorption of 3D orthogonal woven fabric under ballistic penetration of hemispherical-cylindrical projectile, J. Text. Inst. 102 (2011) 875–889. https://doi.org/10.1080/00405000.2010.525815.

[16] K. Bilisik, Two-dimensional (2D) fabrics and three-dimensional (3D) preforms for ballistic and stabbing protection: A review, Text. Res. J. 87 (2016) 2275–2304. https://doi.org/10.1177/0040517516669075.

[17] H. Wang, P.J. Hazell, K. Shankar, E. V. Morozov, Z. Jovanoski, A.D. Brown, Z. Li, J.P. Escobedo-Diaz, Tensile properties of ultra-high-molecular-weight polyethylene

single yarns at different strain rates, J. Compos. Mater. 54 (2020) 1453–1466. https://doi.org/10.1177/0021998319883416.
[18] T.A. Bogetti, M. Walter, J. Staniszewski, J. Cline, Interlaminar shear characterization of ultra-high molecular weight polyethylene (UHMWPE) composite laminates, Compos. Part A Appl. Sci. Manuf. 98 (2017) 105–115. https://doi.org/10.1016/j.compositesa.2017.03.018.
[19] L.H. Nguyen, T.R. Lässig, S. Ryan, W. Riedel, A.P. Mouritz, A.C. Orifici, A methodology for hydrocode analysis of ultra-high molecular weight polyethylene composite under ballistic impact, Compos. Part A Appl. Sci. Manuf. 84 (2016) 224–235. https://doi.org/10.1016/j.compositesa.2016.01.014.
[20] L.F. da Silva, A. Lavoratti, I.M. Pereira, R.R. Dias, S.C. Amico, A.J. Zattera, Development of multilaminar composites for vehicular ballistic protection using ultra-high molecular weight polyethylene laminates and aramid fabrics, J. Compos. Mater. 53 (2019) 1907–1916. https://doi.org/10.1177/0021998318815959.
[21] H. Wang, P.J. Hazell, K. Shankar, E. V. Morozov, J.P. Escobedo, C. Wang, Effects of fabric folding and thickness on the impact behaviour of multi-ply UHMWPE woven fabrics, J. Mater. Sci. 52 (2017) 13977–13991. https://doi.org/10.1007/s10853-017-1482-y.
[22] S. Min, Y. Chu, X. Chen, Numerical study on mechanisms of angle-plied panels for ballistic protection, Mater. Des. 90 (2016) 896–905. https://doi.org/10.1016/j.matdes.2015.11.019.
[23] H. Wang, P.J. Hazell, K. Shankar, E. V. Morozov, J.P. Escobedo, Impact behaviour of Dyneema® fabric-reinforced composites with different resin matrices, Polym. Test. 61 (2017) 17–26. https://doi.org/10.1016/j.polymertesting.2017.04.026.
[24] T.L. Chu, C. Ha-Minh, A. Imad, Analysis of local and global localizations on the failure phenomenon of 3D interlock woven fabrics under ballistic impact, Compos. Struct. 159 (2016) 267–277. https://doi.org/10.1016/j.compstruct.2016.09.039.
[25] M. Xuhong, K. Xiangyong, J. Gaoming, The experimental research on the stab resistance of warp-knitted spacer fabric, J. Ind. Text. 43 (2013) 281–301. https://doi.org/10.1177/1528083712464256.
[26] M. El Messiry, E. Eltahan, Stab resistance of triaxial woven fabrics for soft body armor, J. Ind. Text. 45 (2016) 1062–1082. https://doi.org/10.1177/1528083714551441.
[27] Y. Xu, X. Chen, Y. Wang, Z. Yuan, Stabbing resistance of body armour panels impregnated with shear thickening fluid, Compos. Struct. 163 (2017) 465–473. https://doi.org/10.1016/j.compstruct.2016.12.056.
[28] W. Li, D. Xiong, X. Zhao, L. Sun, J. Liu, Dynamic stab resistance of ultra-high molecular weight polyethylene fabric impregnated with shear thickening fluid, Mater. Des. 102 (2016) 162–167. https://doi.org/10.1016/j.matdes.2016.04.006.
[29] B. Gu, 6-Modelling of 3D woven fabrics for ballistic protection, in: Adv. Fibrous Compos. Mater. Ballist. Prot., Elsevier Ltd, 2016: pp. 145–197. https://doi.org/10.1016/B978-1-78242-461-1.00006-6.
[30] C. Ha-Minh, A. Imad, F. Boussu, T. Kanit, Experimental and numerical investigation of a 3D woven fabric subjected to a ballistic impact, Int. J. Impact Eng. 88 (2015) 91–101. https://doi.org/10.1016/j.ijimpeng.2015.08.011.
[31] B.K. Behera, B.P. Dash, Mechanical behavior of 3D woven composites, Mater. Des. 67 (2014) 261–271. https://doi.org/10.1016/j.matdes.2014.11.020.
[32] M. Wang, M. Cao, H. Wang, A. Siddique, B. Gu, B. Sun, Drop-weight impact behaviors of 3-D angle interlock woven composites after thermal oxidative aging, Compos. Struct. 166 (2017) 239–255. https://doi.org/10.1016/j.compstruct.2017.01.046.
[33] A.K. Dash, B.K. Behera, Role of stuffer layers and fibre volume fractions on the

mechanical properties of 3D woven fabrics for structural composites applications, J. Text. Inst. 110 (2019) 614–624. https://doi.org/10.1080/00405000.2018.1502502.
[34] B.K. Behera, B.P. Dash, An experimental investigation into structure and properties of 3D-woven aramid and PBO fabrics, J. Text. Inst. 104 (2013) 1337–1344. https://doi.org/10.1080/00405000.2013.805873.
[35] P. Wang, B. Sun, B. Gu, Comparison of stab behaviors of uncoated and coated woven fabrics from experimental and finite element analyses, Text. Res. J. 82 (2012) 1337–1354. https://doi.org/10.1177/0040517511418560.
[36] Y. Xu, X. Chen, Y. Wang, Z. Yuan, Stabbing resistance of body armour panels impregnated with shear thickening fluid, Compos. Struct. 163 (2017) 465–473. https://doi.org/10.1016/j.compstruct.2016.12.056.
[37] J. Cheon, M. Lee, M. Kim, Study on the stab resistance mechanism and performance of the carbon , glass and aramid fi ber reinforced polymer and hybrid composites, Compos. Struct. 234 (2020). https://doi.org/10.1016/j.compstruct.2019.111690.
[38] S. Gürgen, T. Yıldız, Stab resistance of smart polymer coated textiles reinforced with particle additives, Compos. Struct. 235 (2020). https://doi.org/10.1016/j.compstruct.2019.111812.
[39] C.S. Li, X.C. Huang, Y. Li, N. Yang, Z. Shen, X.H. Fan, Stab resistance of UHMWPE fiber composites impregnated with thermoplastics, Polym. Adv. Technol. 25 (2014) 1014–1019. https://doi.org/10.1002/pat.3344.
[40] Å. Erlandsson, J. Reid Meloy, The Swedish School Attack in Trollhättan, J. Forensic Sci. 63 (2018) 1917–1927. https://doi.org/10.1111/1556-4029.13800.
[41] N. Radojevi, Multiple stabbing in sex-related homicides, J. Forensic Leg. Med. 20 (2013) 502–507. https://doi.org/10.1016/j.jflm.2013.03.005.
[42] M. Afshari, D.J. Sikkema, K. Lee, M. Bogle, High Performance Fibers Based on Rigid and Flexible Polymers, Polym. Rev. 48 (2008) 230–274. https://doi.org/10.1080/15583720802020129.
[43] M. Li, P. Wang, F. Boussu, D. Soulat, Effect of Fabric Architecture on Tensile Behaviour of the High-Molecular-Weight Polyethylene 3-Dimensional Interlock Composite Reinforcements, Polymers (Basel). 12 (2020) 1–18. https://doi.org/10.3390/polym12051045.
[44] https://www.packagingcomposites-honeywell.com/spectra/product-info/spectra-fiber/, (n.d.).
[45] B. Sun, R. Zhang, Q. Zhang, R. Gideon, B. Gu, Drop-weight impact damage of three-dimensional angle-interlock woven composites, J. Compos. Mater. 47 (2013) 2193–2209. https://doi.org/10.1177/0021998312454904.
[46] L. Gilson, L. Rabet, A. Imad, F. Coghe, Experimental and numerical characterisation of rheological properties of a drop test response of a ballistic plastilina, Forensic Sci. Int. 310 (2020). https://doi.org/10.1016/j.forsciint.2020.110238.
[47] T. Payne, S. O'Rourke, Body Armour Standard (2017) Guidance, 2017.
[48] P. Reiners, Investigation about the stab resistance of textile structures, methods for their testing and improvements, University of Upper Alsace. Ph.D thesis, 2016.
[49] D.T. Tien, J.S. Kim, Y. Huh, Evaluation of anti-stabbing performance of fabric layers woven with various hybrid yarns under different fabric conditions, Fibers Polym. 12 (2011) 808–815. https://doi.org/10.1007/s12221-011-0808-7.
[50] T.T. Li, R. Wang, C.W. Lou, J.H. Lin, Static and dynamic puncture behaviors of compound fabrics with recycled high-performance Kevlar fibers, Compos. Part B Eng. 59 (2014) 60–66. https://doi.org/10.1016/j.compositesb.2013.10.063.
[51] A.N. Annaidh, M. Cassidy, M. Curtis, M. Destrade, M.D. Gilchrist, Toward a predictive assessment of stab-penetration forces, Am. J. Forensic Med. Pathol. 36

(2015) 162–166. https://doi.org/10.1097/PAF.0000000000000075.
[52] I. Horsfall, Stab resistant body armour, Cranfield uniersity. Ph.D thesis, 1999. http://dspace.lib.cranfield.ac.uk/handle/1826/4930.
[53] L. Wang, S. Zhang, W.M. Gao, X. Wang, FEM analysis of knife penetration through woven fabrics, C. - Comput. Model. Eng. Sci. 20 (2007) 11–20. https://doi.org/10.3970/cmes.2007.020.011.
[54] A.A. Johnson, Establishing design characteristics for the development of stab resistant Laser Sintered body armour, Loughborough University. Ph.D thesis, 2014.
[55] S.M. Hejazi, N. Kadivar, A. Sajjadi, Analytical assessment of woven fabrics under vertical stabbing – The role of protective clothing, Forensic Sci. Int. 259 (2016) 224–233. https://doi.org/10.1016/j.forsciint.2015.12.036.
[56] Y.H. Duong Tu Tien, Jong S. Kim, Stab-resistant property of the fabrics woven with the aramid/cotton core-spun yarns, Fibers Polym. 11 (2010) 500–506. https://doi.org/10.1007/s12221-010-0500-3.
[57] H. Shen, P. Wang, X. Legrand, L. Liu, Characterisation and optimisation of wrinkling during the forming of tufted three-dimensional composite preforms, Compos. Part A Appl. Sci. Manuf. 127 (2019) 105651. https://doi.org/10.1016/j.compositesa.2019.105651.
[58] N. Aspert, D. Santa-Cruz, T. Ebrahimi, MESH: Measuring errors between surfaces using the Hausdorff distance, in: Proc. - 2002 IEEE Int. Conf. Multimed. Expo, ICME 2002, 2002: pp. 705–708. https://doi.org/10.1109/ICME.2002.1035879.
[59] M. Li, P. Wang, Dynamic stab resistance of multi-ply three-dimensional warp interlock fabrics with polyethylene yarns for protective applications, J. Ind. Text. (2020). https://doi.org/10.1177/1528083720965685.
[60] M. El Messiry, Investigation of puncture behaviour of flexible silk fabric composites for soft body armour, Fibres Text. East. Eur. 22 (2014) 71–76.
[61] D. Tabor, The harness of metal, in: Clarendon Press, Oxford, 1951: pp. 95–114.
[62] O. Rozant, P.E. Bourban, J.A.E. Månson, Drapability of dry textile fabrics for stampable thermoplastic preforms, Compos. Part A Appl. Sci. Manuf. 31 (2000) 1167–1177. https://doi.org/10.1016/S1359-835X(00)00100-7.
[63] M.V. Hosur, J.B. Mayo Jr., E. Wetzel, S. Jeelani, Studies on the fabrication and stab resistance characterization ofnovel thermoplastic-kevlar composites, Solid State Phenom. 136 (2008) 83–92. https://doi.org/10.4028/www.scientific.net/SSP.136.83.

Stabbing impact in single and double pass cases